

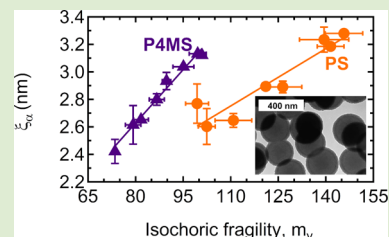
# Characteristic Length of the Glass Transition in Isochorically Confined Polymer Glasses

Chuan Zhang,<sup>†</sup> Yunlong Guo,<sup>†</sup> and Rodney D. Priestley<sup>\*,†,‡</sup>

<sup>†</sup>Department of Chemical and Biological Engineering and <sup>‡</sup>Princeton Institute for the Science and Technology of Materials, Princeton University, Princeton, New Jersey 08544, United States

## Supporting Information

**ABSTRACT:** We report the effect of isochoric confinement on the characteristic length of the glass transition ( $\xi_\alpha$ ) for polystyrene (PS) and poly(4-methylstyrene) (P4MS). Utilizing silica-capped PS and P4MS nanoparticles as model systems,  $\xi_\alpha$  values are determined from the thermal fluctuation model and calorimetric data. With decreasing nanoparticle diameter,  $\xi_\alpha$  decreases, suggesting a reduction in the number of segmental units required for cooperative motion at the glass transition under confinement. Furthermore, a direct correlation is observed between  $\xi_\alpha$  and the isochoric fragility ( $m_v$ ) in confined polymers. Due to a nearly constant ratio of the isochoric to isobaric fragility in confined polymer nanoparticles, a correlation between  $\xi_\alpha$  and  $m_v$  also implies a correlation between  $\xi_\alpha$  and the volume contribution to the temperature dependence of structural relaxation. Lastly, we observe that when the fragility and characteristic length are varied in the same system the relationship between the two properties appears to be more correlated than that of across different bulk glass-formers.



Polymers under nanoscale confinement can exhibit dramatic changes in glassy properties relative to the bulk. For polystyrene (PS), reductions in the glass transition temperature ( $T_g$ ) have been observed in a range of confined geometries, including supported thin films,<sup>1</sup> freestanding thin films,<sup>2</sup> nanocomposites,<sup>3</sup> and nanoparticles.<sup>4,5</sup> While significant interest and debate about the origins and existence of  $T_g$  deviations with confinement still remain,<sup>6</sup> one way to increase our understanding of glassy behavior in confined polymers is to examine other manifestations of the glass transition, e.g., the fragility. The fragility ( $m$ ) describes the steepness of the temperature ( $T$ ) dependence of the cooperative segmental relaxation time ( $\tau$ ) at  $T_g$  and is mathematically defined as<sup>7,8</sup>

$$m = \left[ \frac{d \log \tau}{d(T_g/T)} \right]_{T=T_g} \quad (1)$$

Glass-formers with high  $m$ -values, e.g., PS ( $m = 150$ ),<sup>9</sup> display a large rate of increase in relaxation time as temperature is reduced toward  $T_g$ .

A classical theory to explain the rapid increase in cooperative segmental relaxation time as  $T_g$  is approached from higher temperatures is the Adam–Gibbs (AG) theory.<sup>10</sup> The central feature of the AG theory is a growing length scale ( $\xi$ ) required for cooperative segmental motion or rearrangement, as  $T$  is decreased toward  $T_g$ . An increase in the cooperative length increases the number of molecules or segmental units ( $z$ ) in a hypothesized cooperatively rearranging region (CRR), which is reflected in a loss of configurational entropy. From the AG theory, the cooperative segmental relaxation time can be related to  $z$  in a CRR<sup>11</sup>

$$\tau = \tau_\infty \exp\left(\frac{zE_\infty}{T}\right) \quad (2)$$

where  $\tau_\infty$  and  $E_\infty$  are constants, representing the high- $T$  relaxation time and activation energy, respectively. In eq 2,  $z$  is a function of  $T$ ; hence, the temperature-dependent activation energy,  $E(T)$ , is equal to  $z(T)E_\infty$ . Combining eqs 1 and 2, a relationship between the fragility and the CRR size, as represented by  $z$ , can be obtained<sup>12</sup>

$$m = \frac{E_\infty}{T_g} z(T_g) - E_\infty \left. \frac{dz}{dT} \right|_{T_g} \quad (3)$$

Here, the AG theory suggests that the fragility should correlate with both the size of a CRR at  $T_g$ , i.e., the characteristic length of the glass transition ( $\xi_\alpha$ ), and the rate of change in  $\xi_\alpha$  with temperature at  $T_g$ .

Experimental studies on various types of bulk glass-formers have suggested that a simple correlation between the fragility and  $\xi_\alpha$  may not exist.<sup>13–16</sup> For instance, Qiu and co-workers observed no obvious trend between the two quantities across four glass-forming materials, i.e., glycerol, *o*-terphenyl, sorbitol, and poly(vinyl acetate).<sup>13</sup> The lack of correlation between fragility and  $\xi_\alpha$  may be due to the second term on the right-hand side of eq 3 describing the rate of change of the extent of cooperative motion. That is, the contribution from this term has been shown to be more important than  $z(T_g)$  in causing changes in the fragility value.<sup>11</sup>

Received: April 6, 2014

Accepted: May 7, 2014

Published: May 13, 2014

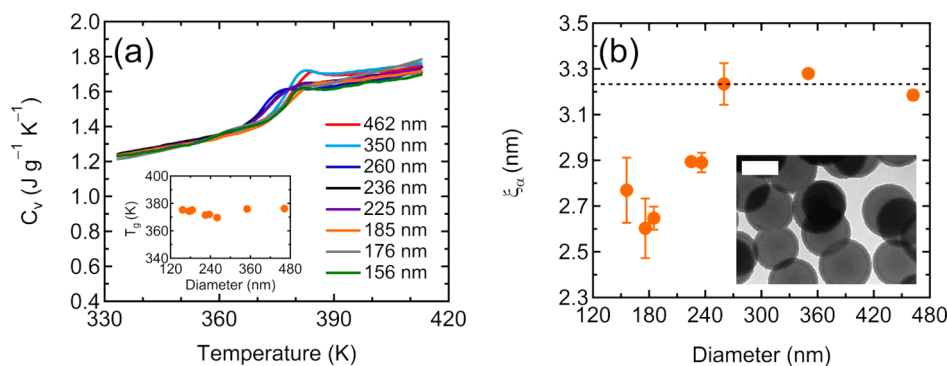


**Figure 1.** (a) DSC traces of silica-capped PS nanoparticles with diameters ranging from 156 to 462 nm. Inset plots the midpoint  $T_g$  vs nanoparticle diameter. (b)  $\xi_\alpha$  as a function of diameter for PS. The dotted line represents the bulk  $\xi_\alpha$  value for PS (3.23 nm), determined by averaging  $\xi_\alpha$  values of nanoparticles exhibiting bulk behavior, i.e.,  $d > 250$  nm. Error bars represent standard deviations of repeated measurements. Inset shows a representative transmission electron microscopy (TEM) image of silica-capped 236 nm diameter PS nanoparticles (scale bar equals 200 nm).

Nevertheless, Sokolov and co-workers recently showed that across various types of bulk glass-formers the characteristic length of the glass transition correlated directly with the volume contribution to the temperature dependence of structural relaxation.<sup>14,15</sup> That is, under isobaric conditions, cooling of the polymer toward  $T_g$  results in a reduction in both thermal energy and specific volume.<sup>17–19</sup> Hence, the rapid change in dynamics near the glass transition is governed by a combination of thermal and volume effects, and the isobaric fragility ( $m_p$ ) can be written in terms of the two effects<sup>17,19</sup>

$$m_p = \left( \frac{\partial \log \tau}{\partial (T_g/T)} \right)_V + \left( \frac{\partial \log \tau}{\partial V} \right)_T \left( \frac{\partial V}{\partial (T_g/T)} \right)_P \quad (T = T_g) \quad (4)$$

where  $V$  is the volume and  $P$  is the pressure. The first term on the right-hand side of eq 4 is simply the definition of the isochoric fragility ( $m_v$ ), which describes the effect of thermal activation on dynamics as  $T_g$  is approached. The second term ( $m_p - m_v$ ) describes the effect of volume on dynamics, as both  $T$  and  $P$  are held constant. We note that it is this term which is proposed to correlate with  $\xi_\alpha$ , at least across different types of bulk glass-formers.<sup>14–16</sup>

In this Letter, we examine the isochoric fragility and the characteristic length of the glass transition in confined polymers to explore correlations between the two properties within the *same system*. We have recently shown that both isobaric and isochoric fragilities decrease with decreasing diameter for polymers confined in the nanoparticle geometry.<sup>9,20</sup> However, the question remains as to whether a corresponding change in the characteristic length at  $T_g$  exists for confined systems.<sup>11,12</sup> In this study, we utilize differential scanning calorimetry (DSC) and the thermal fluctuation model (eq 5) to determine the characteristic length of the glass transition for polymers under isochoric confinement. For the case of silica-capped PS and poly(4-methylstyrene) (P4MS) nanoparticles, we show that  $\xi_\alpha$  decreases with increasing confinement, i.e., with decreasing diameter ( $d$ ). Hence, a strong correlation between  $\xi_\alpha$  and  $m_v$  in confined polymers is reported for the first time. Furthermore, given the unique geometry of silica-capped polymer nanoparticles, a correlation between  $\xi_\alpha$  and  $m_v$  also implies a correlation between  $\xi_\alpha$  and  $m_p - m_v$ , as detailed below. The results are discussed in the context of the Adam–Gibbs theory and compared with recent works correlating fragility and CRR

size across various types of bulk glass-formers<sup>14–16</sup> and in layered thin films.<sup>21</sup>

Monodisperse PS and P4MS nanoparticles with diameters ranging from 110 to 630 nm were synthesized using surfactant-free emulsion polymerization.<sup>4,9,20</sup> Subsequently, the bare PS and P4MS nanoparticles were coated with a  $\sim 30$  nm thick silica shell via a modified Stöber method.<sup>9,20,22,23</sup> Silica capping of the polymer nanoparticles resulted in isochoric conditions, as previously shown by comparing the heat capacity jump at  $T_g$  for the silica-capped samples to bare nanoparticles or the bulk.<sup>9,20,24</sup> The synthesized silica-capped nanoparticles were dried under the hood overnight and subsequently annealed under vacuum at 353 K for at least 24 h. Thermal measurements were conducted using DSC (TA Instruments Q2000) at constant cooling and heating rates of 10 K/min. The Supporting Information provides details on relevant characterization techniques.

While several experimental techniques, including light scattering<sup>14</sup> and 4-D nuclear magnetic resonance (NMR),<sup>13</sup> have been used in determining cooperative length scales in various glass-formers, an alternative method to calculate  $\xi_\alpha$  was derived by Donth<sup>25,26</sup> based on thermal fluctuations in compact subsystems.<sup>27</sup> According to Donth's approach,  $\xi_\alpha$  can be determined from the  $T_g$ , the isochoric heat capacity ( $C_v$ ), the density of the glass-former ( $\rho$ ), and the mean temperature fluctuations across the CRR volume ( $\delta T$ ), which is related to the breadth of the glass transition, as follows

$$\xi_\alpha = \left[ \frac{k_B T_g^2 \Delta(1/C_v)}{\rho (\delta T)^2} \right]^{1/3} \quad (5)$$

Here,  $k_B$  is the Boltzmann constant and  $\Delta(1/C_v)$  is equal to  $1/C_{v,\text{glass}}(T_g) - 1/C_{v,\text{liquid}}(T_g)$ . Utilizing calorimetric techniques, e.g., DSC or modulated differential scanning calorimetry (MDSC), the parameters  $C_v$ ,  $T_g$ , and  $\delta T$  can be determined in a single experiment. In previous studies, eq 5 has been used to calculate  $\xi_\alpha$  in bulk glass-formers, i.e., small molecules<sup>28</sup> and polymers,<sup>16,26,28–31</sup> as well as small molecules confined in nanopores<sup>32</sup> and polymers confined in the nanocomposite geometry.<sup>33</sup>

To confirm the thermal fluctuation model in determining the characteristic length of the glass transition to systems investigated here, eq 5 was first applied to a series of commercially obtained (Sigma-Aldrich or Scientific Polymer) bulk PS with  $M_w$  ranging from 1.14 to 250 kg/mol. Detailed

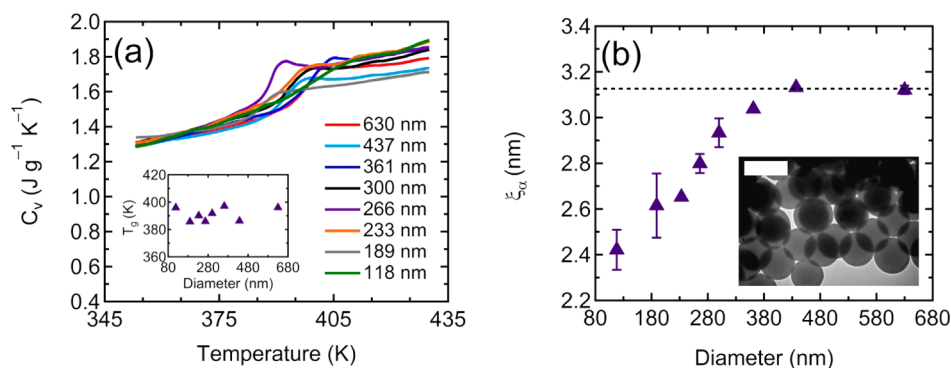


**Figure 2.** (a) DSC traces of silica-capped P4MS nanoparticles with diameters ranging from 118 to 630 nm. Inset plots the midpoint  $T_g$  vs nanoparticle diameter. (b)  $\xi_\alpha$  as a function of diameter for P4MS. The dotted line represents the bulk  $\xi_\alpha$  value for P4MS (3.13 nm), determined by averaging  $\xi_\alpha$  values of nanoparticles exhibiting bulk behavior, i.e.,  $d > 430$  nm. Error bars represent standard deviations of repeated measurements. Inset shows a representative TEM image of silica-capped 361 nm diameter P4MS nanoparticles (scale bar equals 500 nm).

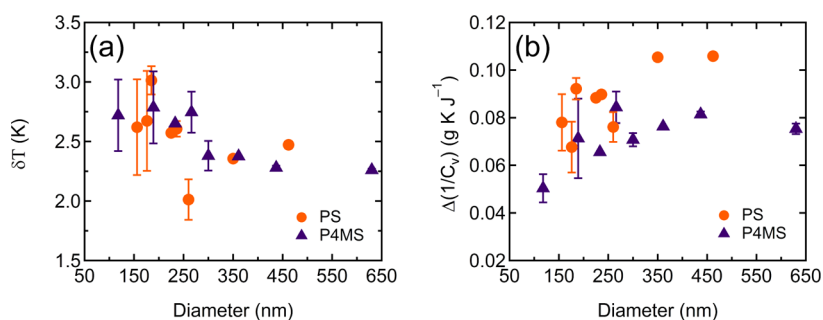


**Figure 3.** (a)  $\delta T$  and (b)  $\Delta(1/C_v)$  as a function of nanoparticle diameter for silica-capped PS (circles) and P4MS (triangles). Error bars represent standard deviations from repeated measurements.

results are highlighted in the Supporting Information (Figures S1 and S2). As the PS  $M_w$  is reduced from 250 to 1.14 kg/mol,  $\xi_\alpha$  decreases from 3.7 to 2.9 nm. The absolute  $\xi_\alpha$  values (and the trend with  $M_w$ ) determined from Donth's approach are in agreement with that from an alternative technique.<sup>14</sup>

Figure 1(a) shows DSC thermograms for silica-capped PS nanoparticles with diameters ranging from 156 to 462 nm, in which the isochoric heat capacity,  $C_v$ , is plotted vs temperature. We note that the PS  $M_w$  for all nanoparticle samples ranges from 100 to 400 kg/mol with a polydispersity index (PDI) of  $\sim 3$ . Here, no systematic deviation (within experimental error) in the midpoint  $T_g$  as a function of nanoparticle diameter is observed (Figure 1(a) inset), in agreement with previous works.<sup>4,9,24</sup> By capping bare PS nanoparticles with a rigid silica shell of  $\sim 30$  nm in thickness (Figure 1(b) inset), isochoric conditions are established.<sup>9</sup> Due to the unique geometry of silica-capped nanoparticles, the isochoric heat capacity,  $C_v$ , is then directly measured via DSC and can be used without further approximations in the thermal fluctuation model.

Figure 1(b) shows the characteristic length of the glass transition as a function of nanoparticle diameter calculated from eq 5 using  $T_g$ ,  $\Delta(1/C_v)$ , and  $\delta T$  values extracted from the calorimetric data presented in Figure 1(a). Here,  $T_g$  is taken as the midpoint temperature between the extrapolated liquid and glassy lines, and  $\delta T$  is determined as  $\delta T = \Delta T/2.5$ , where  $\Delta T$  represents the temperature interval in which the isochoric heat capacity varies between 16% and 84% of the total heat capacity jump at  $T_g$  ( $\Delta C_v$ ).<sup>28,31</sup> The dotted line represents the bulk  $\xi_\alpha$  value for PS (= 3.23 nm), determined by averaging  $\xi_\alpha$  values of silica-capped PS nanoparticles which exhibit bulk behavior, i.e.,  $d > 250$  nm. A bulk  $\xi_\alpha$  value of 3.23 nm is in close agreement

with the size of CRR for bulk PS  $M_w = 233$  kg/mol ( $\xi_\alpha = 3.38$  nm) determined using the frequency of the boson peak and the transverse sound velocity.<sup>14</sup> As shown in Figure 1(b), when the nanoparticle diameter is reduced from 462 to 156 nm,  $\xi_\alpha$  decreases from the bulk value of 3.23 to 2.77 nm. The onset diameter in which a reduction in  $\xi_\alpha$  is observed for silica-capped PS is  $\sim 260$  nm, which is equivalent to the onset diameter at which a reduction in the isochoric fragility was observed in silica-capped PS nanoparticles.<sup>9</sup>

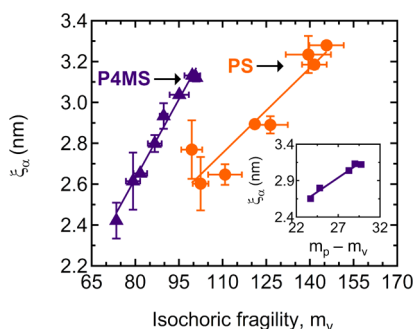
To examine the effect of chemical structure on the observed  $\xi_\alpha$ -confinement effect, calorimetry is conducted on silica-capped P4MS nanoparticles with diameters ranging from 118 to 630 nm as shown in Figure 2(a), in which the isochoric heat capacity is plotted vs temperature. We note that the P4MS  $M_w$  for all nanoparticle samples ranges from 40 to 400 kg/mol with a PDI of  $\sim 3$ . The difference between the chemical structures of PS and the P4MS is the addition of a methyl group on the 4-position of the phenyl ring for P4MS. As shown in Figure 2(a) inset, the midpoint  $T_g$  does not deviate systematically (within experimental error) for P4MS with decreasing nanoparticle diameter, in agreement with previous results<sup>20</sup> and the results of silica-capped PS nanoparticles. Here, the absolute  $T_g$  of P4MS is  $\sim 10$  K higher than PS due to the fact that the alkyl substituent on the phenyl ring increases the bulkiness of the repeat unit, which reduces segmental mobility and causes an increase in  $T_g$ .<sup>34</sup>

Figure 2(b) plots the calculated  $\xi_\alpha$  for P4MS as a function of nanoparticle diameter using  $T_g$ ,  $\Delta(1/C_v)$ , and  $\delta T$  values extracted from the calorimetric data presented in Figure 2(a). The dotted line represents the bulk  $\xi_\alpha$  value for P4MS (= 3.13 nm), determined by averaging  $\xi_\alpha$  values of nanoparticles

exhibiting bulk behavior, i.e.,  $d > 430$  nm, which is in agreement with the literature value.<sup>29</sup> In Figure 2(b), as the diameter is decreased from 630 to 118 nm for P4MS,  $\xi_\alpha$  decreases from the bulk value of 3.13 to 2.42 nm. Furthermore, the onset diameter at which a reduction in the characteristic length of the glass transition occurs is  $\sim 420$  nm. Analogous to the case of silica-capped PS nanoparticles, the onset diameter of a reduction in  $\xi_\alpha$  in P4MS is equivalent to the diameter at which a reduction in the isochoric fragility was observed to occur in silica-capped P4MS nanoparticles.<sup>20</sup> A larger onset diameter of  $\sim 420$  nm for P4MS, as compared to PS ( $\sim 260$  nm), in the  $\xi_\alpha$ -confinement effect may be a result of a more pronounced effect of the linear alkyl as flexible spacers in confined systems.<sup>34</sup>

In both silica-capped PS and P4MS, we observe a reduction in  $\xi_\alpha$  as nanoparticle diameter is decreased. A reduction in  $\xi_\alpha$  suggests that the number of segmental units ( $z$ ) required for cooperative motion at  $T_g$  is reduced as PS and P4MS become more isochorically confined in the nanoparticle geometry. We note that since the  $T_g$  of PS and P4MS does not deviate systematically with nanoparticle diameter a reduction in  $\xi_\alpha$  is then caused by an apparent increase and decrease in  $\delta T$  and  $\Delta(1/C_v)$ , respectively, with confinement, as shown in Figure 3. An increase in  $\delta T$  implies a broadening of the glass transition event, i.e., a wider temperature range in which the glass transition takes place. A broader glass transition can be understood as a result of a reduced mobile layer at the polymer/silica interface, and the effect is more pronounced as the nanoparticle diameter is reduced (due to an increase in the surface area to volume ratio). The results are consistent with previous observations of a broadening of the relaxation peak toward higher temperatures in variable cooling rate DSC measurements of silica-capped PS and P4MS nanoparticles for the smaller diameters at the lower cooling rates.<sup>9,20</sup> Furthermore, a decrease in  $\Delta(1/C_v)$  with confinement may also be a consequence of the reduced mobile layer.

Figure 4 examines the relationship between  $\xi_\alpha$  and  $m_v$  for polymers under confinement. Here, a linear correlation



**Figure 4.**  $\xi_\alpha$  as a function of the isochoric fragility,  $m_v$ , for both silica-capped PS (circles) and P4MS (triangles) nanoparticles. Values of the isochoric fragility are taken from refs 9 and 20. Inset shows  $\xi_\alpha$  vs  $m_p - m_v$ , i.e., the volume contribution to the temperature dependence of structural relaxation, for P4MS, where the isobaric fragility,  $m_p$ , is taken from ref 20. Solid lines are linear fits to the experimental data, and error bars represent standard deviations from repeated measurements.

between  $\xi_\alpha$  and  $m_v$  is observed for both silica-capped PS and P4MS nanoparticles, which is a key result of the current study. The values of  $m_v$  are taken from refs 9 and 20 in which variable cooling rate DSC was utilized to determine the fragility of silica-capped polymers. While recent studies in the literature have revealed no clear correlation between  $\xi_\alpha$  and  $m_p$  (or  $m_v$ )

across various types of bulk glass-formers,  $\xi_\alpha$  has been observed to correlate linearly to the volume contribution to the temperature dependence of structural relaxation, i.e.,  $m_p - m_v$ .<sup>14–16</sup> For polymer nanoparticles, we have shown previously that the relative contribution of thermal effects to changes in dynamics as  $T_g$  is approached, i.e., the ratio  $m_v/m_p$ , remains nearly constant with increasing confinement.<sup>20</sup> A nearly constant  $m_v/m_p$  value with confinement implies that the volume contribution to the temperature dependence of structural relaxation, or  $m_p - m_v$ , should also decrease proportionally with a decrease in  $m_v$  in confined polymer. In other words,  $m_v$  is proportional to  $m_p - m_v$  for all polymer nanoparticle diameters. Hence, if  $\xi_\alpha$  correlates linearly to  $m_v$ , as shown in Figure 4 for PS and P4MS, then  $\xi_\alpha$  should also correlate linearly to  $m_p - m_v$ . A correlation between  $\xi_\alpha$  and  $m_p - m_v$  is clearly observed in the inset of Figure 4 for silica-capped P4MS nanoparticles, consistent with the observation that  $\xi_\alpha$  correlates with  $m_p - m_v$  across various types of bulk glass-formers.<sup>14–16</sup> Furthermore, in a recent experimental study by Arabeche and co-workers on layered polycarbonate (PC)/poly(methyl methacrylate) (PMMA) films,  $\xi_\alpha$  was found to correlate linearly with both  $m_p$  and  $m_p - m_v$  in PC as the layer thickness was reduced from 16  $\mu\text{m}$  to 12 nm.<sup>21</sup> Similarly, for bulk PS of varying  $M_w$ ,  $m_p$  was found to be linearly correlated to  $\xi_\alpha$ .<sup>14</sup> It is intriguing to note that those results and the results of the current study suggest that for systems in which the fragility and characteristic length are varied within the *same system* (either through confinement or  $M_w$ ) the relationship between fragility and  $\xi_\alpha$  appears to be more correlated when compared to that of across various types of bulk glass-formers.

An interesting and unique observation in the current study is that while both  $m_v$  and  $\xi_\alpha$  decrease with increasing confinement in silica-capped polymer nanoparticles the  $T_g$  remains invariant (Figures 1(a) and 2(a) insets). In the context of the Adam–Gibbs theory, the fragility should be a function of  $z(T_g)$  (or  $\xi_\alpha$ ),  $dz/dT$  at  $T_g$ ,  $E_\infty$ , and the  $T_g$ , as shown in eq 3. Hence, if the  $T_g$  is constant and both  $z(T_g)$  and fragility are reduced with confinement, one implication from the AG theory is that  $E_\infty$  must also remain constant with confinement. As a result, for the  $T_g$  to be constant while  $z(T_g)$  decreases at  $\tau = 100$  s, the prefactor,  $\tau_\infty$ , in eq 2 must increase with confinement. Alternatively, if  $\tau_\infty$  is to remain constant, then the  $E_\infty$  value must grow with increasing confinement to compensate for a shrinking  $z(T_g)$  to get the same  $T_g$ . In this scenario, when  $T_g$  is constant while  $E_\infty$  increases and  $z(T_g)$  decreases, the first term on the right-hand side of eq 3 is more or less constant; hence, the only term which will contribute to the decrease in fragility with confinement observed in the current work is the  $dz/dT$  term. Currently, the exact scenario in which our results satisfy the AG theory cannot be confirmed. However, future experiments using frequency-based techniques, e.g., dielectric relaxation spectroscopy, may shed more light. Lastly, we note that in recent computational studies on polymer nanocomposites it has been shown that the change in the  $dz/dT$  term with confinement contributes to the fragility much more than the size of the CRR itself.<sup>11,12</sup>

In summary, the characteristic length of the glass transition,  $\xi_\alpha$ , was calculated using the thermal fluctuation model proposed by Donth<sup>25,26</sup> for a series of silica-capped PS and P4MS nanoparticle samples with diameters ranging from 118 to 630 nm. In both cases, with increasing the degree of isochoric confinement, i.e., decreasing nanoparticle diameter,  $\xi_\alpha$  was found to decrease below an onset diameter. We then showed

that  $\xi_\alpha$  correlated directly to the isochoric fragility,  $m_v$ , under confinement. Furthermore, the observed correlation between  $\xi_\alpha$  and  $m_v$  in confined polymer was found to be consistent with the correlation of  $\xi_\alpha$  and  $m_p - m_v$  observed across various types of bulk glass-formers<sup>14–16</sup> and with layered thin films.<sup>21</sup>

## ■ ASSOCIATED CONTENT

### ■ Supporting Information

Full characterization details and application of the thermal fluctuation model toward bulk polymers are given. This material is available free of charge via the Internet at <http://pubs.acs.org>.

## ■ AUTHOR INFORMATION

### Corresponding Author

\*E-mail: [rpriestl@princeton.edu](mailto:rpriestl@princeton.edu).

### Notes

The authors declare no competing financial interest.

## ■ ACKNOWLEDGMENTS

We acknowledge usage of the PRISM Imaging and Analysis Center, which is supported in part by the NSF MRSEC program through the Princeton Center for Complex Materials (DMR-0819860). C.Z. acknowledges support by the Department of Defense (DoD) through the National Defense Science & Engineering Graduate Fellowship (NDSEG). R.D.P. acknowledges the donors of the American Chemical Society Petroleum Research Fund (PRF 49903-DNI10) and the 3M-nontenured faculty grant program for partial support of this work.

## ■ REFERENCES

- (1) Ellison, C. J.; Torkelson, J. M. *Nat. Mater.* **2003**, *2*, 695–700.
- (2) Forrest, J. A.; Dalnoki-Veress, K.; Stevens, J. R.; Dutcher, J. R. *Phys. Rev. Lett.* **1996**, *77*, 2002–2005.
- (3) Bansal, A.; Yang, H. C.; Li, C. Z.; Cho, K. W.; Benicewicz, B. C.; Kumar, S. K.; Schadler, L. S. *Nat. Mater.* **2005**, *4*, 693–698.
- (4) Zhang, C.; Guo, Y.; Priestley, R. D. *Macromolecules* **2011**, *44*, 4001–4006.
- (5) Feng, S.; Li, Z.; Liu, R.; Mai, B.; Wu, Q.; Liang, G.; Gao, H.; Zhu, F. *Soft Matter* **2013**, *9*, 4614–4620.
- (6) Tress, M.; Erber, M.; Mapesa, E. U.; Huth, H.; Muller, J.; Serghei, A.; Schick, C.; Eichhorn, K. J.; Volt, B.; Kremer, F. *Macromolecules* **2010**, *43*, 9937–9944.
- (7) Angell, C. A. *Science* **1995**, *267*, 1924–35.
- (8) Qin, Q.; McKenna, G. B. *J. Non-Cryst. Solids* **2006**, *352*, 2977–2985.
- (9) Zhang, C.; Guo, Y.; Shepard, K. B.; Priestley, R. D. *J. Phys. Chem. Lett.* **2013**, *4*, 431–436.
- (10) Adam, G.; Gibbs, J. H. *J. Chem. Phys.* **1965**, *43*, 139.
- (11) Starr, F. W.; Douglas, J. F. *Phys. Rev. Lett.* **2011**, *106*, 115702.
- (12) Pazmiño Betancourt, B. A.; Douglas, J. F.; Starr, F. W. *Soft Matter* **2013**, *9*, 241–254.
- (13) Qiu, X. H.; Ediger, M. D. *J. Phys. Chem. B* **2003**, *107*, 459–464.
- (14) Hong, L.; Gujrati, P. D.; Novikov, V. N.; Sokolov, A. P. *J. Chem. Phys.* **2009**, *131*, 194511.
- (15) Hong, L.; Novikov, V. N.; Sokolov, A. P. *J. Non-Cryst. Solids* **2011**, *357*, 351–356.
- (16) Bouthegourd, E.; Esposito, A.; Lourdin, D.; Saiter, A.; Saiter, J. M. *Phys. B: Condens. Matter* **2013**, *425*, 83–89.
- (17) Niss, K.; Dalle-Ferrier, C.; Tarjus, G.; Alba-Simionesco, C. *J. Phys.: Condens. Matter* **2007**, *19*, 076102.
- (18) Casalini, R.; Roland, C. M. *Phys. Rev. E* **2005**, *72*, 031503.

(19) Floudas, G.; Paluch, M.; Grzybowski, A.; Ngai, K. *Molecular Dynamics of Glass-Forming Systems*, 1st ed.; Springer: Heidelberg, Germany, 2011.

(20) Zhang, C.; Priestley, R. D. *Soft Matter* **2013**, *9*, 7076–7085.

(21) Arabeche, K.; Delbreilh, L.; Saiter, J. M.; Michler, G. H.; Adhikari, R.; Baer, E. *Polymer* **2014**, *55*, 1546–1551.

(22) Graf, C.; Vossen, D. L. J.; Imhof, A.; van Blaaderen, A. *Langmuir* **2003**, *19*, 6693–6700.

(23) Zhang, L.; D'Acunzi, M.; Kappl, M.; Auernhammer, G. K.; Vollmer, D.; van Kats, C. M.; van Blaaderen, A. *Langmuir* **2009**, *25*, 2711–2717.

(24) Guo, Y.; Zhang, C.; Lai, C.; Priestley, R. D.; D'Acunzi, M.; Fytas, G. *ACS Nano* **2011**, *5*, 5365–73.

(25) Donth, E. *J. Non-Cryst. Solids* **1982**, *53*, 325–330.

(26) Donth, E. *J. Polym. Sci., Part B: Polym. Phys.* **1996**, *34*, 2881–2892.

(27) Donth's approach assumes that cooperativity (and the hypothesized CRR) takes on the form of compact objects. However, it must be noted that most simulation and modeling studies show that the cooperative units are more ramified.

(28) Hempel, E.; Hempel, G.; Hensel, A.; Schick, C.; Donth, E. *J. Phys. Chem. B* **2000**, *104*, 2460–2466.

(29) Ellison, C. J.; Mundra, M. K.; Torkelson, J. M. *Macromolecules* **2005**, *38*, 1767–1778.

(30) Lixon, C.; Delpouve, N.; Saiter, A.; Dargent, E.; Grohens, Y. *Eur. Polym. J.* **2008**, *44*, 3377–3384.

(31) Grigoras, C. V.; Grigoras, A. G. *J. Therm. Anal. Calorim.* **2011**, *103*, 661–668.

(32) Hempel, E.; Huwe, A.; Otto, K.; Janowski, F.; Schroter, K.; Donth, E. *Thermochim. Acta* **1999**, *337*, 163–168.

(33) Tran, T. A.; Said, S.; Grohens, Y. *Macromolecules* **2005**, *38*, 3867–3871.

(34) Kunal, K.; Robertson, C. G.; Pawlus, S.; Hahn, S. F.; Sokolov, A. P. *Macromolecules* **2008**, *41*, 7232–7238.